  Bull. Chem, Soc. Jpn., 56, 1761—1767 (1983)

Electrochemical Oxidation and Reduction of Flavin-Adenine Dinucleotide Adsorbed on a Mercury Electrode Surface

Tadaaki KAKUTANI, Isao KATASHO, and Mitsugi SENDA
Department of Agricultural Chemistry, Faculty of Agriculture, Kyoto University, Sakyo-ku, Kyoto 606
(Received December 23, 1982)

The electrochemical redox reaction of flavin–adenine dinucleotide (FAD) adsorbed on a hanging mercury drop electrode was studied in a pH 6.9 phosphate buffer by means of cyclic d.c. and a.c. voltammetry. Both the oxidized and reduced forms of FAD were strongly adsorbed on the mercury electrode surface. At the surface concentrations of FAD, Γ, lower than 5.0×10^{-11} mol cm^{-2}, the cyclic d.c. and a.c. voltammetric behavior of adsorbed FAD was explained by the theory for a two-step one-electron surface redox reaction. The formal redox potential, semiquinone formation constant, and charge transfer rate constant for the surface redox reaction of FAD and the interaction parameter of adsorbed FAD species were determined. Cyclic d.c. voltammetry and differential capacity measurement showed that, as Γ exceeded 5×10^{-11} mol cm^{-2}, the reorientation of adsorbed FAD molecules occurred. At $\Gamma>5.8\times10^{-11}$ mol cm^{-2}, the semiquinone formation constant was very small and the behavior was interpreted by the theory of a single-step two-electron surface redox reaction. The electrochemical surface redox properties of FAD adsorbed on a mercury electrode surface appear to depend on the orientation mode of adsorbed FAD molecules.

In a previous paper[1] we have shown that a stable adsorption monolayer of flavin mononucleotide (FMN) is formed on a mercury electrode surface and that the electrochemical redox reaction of the adsorbed FMN is well explained by the theory of a two-step one-electron surface redox reaction. The apparent charge transfer rate constants, redox potentials, and semiquinone formation constants of the surface redox reaction have been determined at pH 6.9 and 4.9 using cyclic d.c. and a.c. voltammetry. Recently the electrochemical behavior of flavin–adenine dinucleotide (FAD) irreversibly adsorbed on graphite and glassy carbon electrode has been studied by Gorton and Johansson[2] and Huck[3,4] using cyclic d.c. voltammetry. The (apparent) charge transfer rate constant of *ca.* 1 s^{-1} for FAD adsorbed on graphite electrode at pH 1.05[2] and the semiquinone formation constant of 2.6 for FAD adsorbed on glassy carbon electrode at pH 7[3] are reported. The charge transfer rate constant obtained by the former authors is considerably smaller compared with that for FMN adsorbed on a mercury electrode,[1] though the isoalloxazine moiety is oxidized or reduced in both the redox reactions of the adsorbed FMN and FAD. It seems interesting to determine the charge transfer rate constant of FAD adsorbed on a mercury electrode and to compare the results with those obtained with FAD adsorbed on a carbon electrode and to elucidate whether the difference, if any, should be ascribed to the difference in the electrode material.

In this work the electrochemical redox reaction of FAD adsorbed on a hanging mercury drop electrode has been studied in a pH 6.9 phosphate buffer by means of cyclic d.c. and a.c. voltammetry. We have determined the kinetic and equilibrium parameters of the surface redox reaction of FAD at the various surface concentrations and found that the charge transfer rate constant and the semiquinone formation constant depend on the orientation mode of the adsorbed FAD molecules. The results and discussion are presented here.

Experimental

Flavin–adenine dinucleotide (FAD) and other chemicals were commercially-available reagent grade materials and were used as received.

All voltammetric measurements were performed in a dark box at 25 °C under potentiostatic conditions with a three-electrode system consisting of a hanging mercury drop working electrode, a coiled platinum counter electrode, and a saturated calomel reference electrode (SCE). The hanging mercury drop electrode (HMDE) was a Metrohm drop electrode E410, the surface area being 0.0187 ± 0.0003 cm^2. Buffer solution containing 0.2 mol dm^{-3} sodium dihydrogenphosphate–disodium hydrogenphosphate of pH 6.9 was used as the base solution. The ionic strength was adjusted to 0.5 mol dm^{-3} with potassium nitrate. D.c. and a.c. voltammograms were recorded after a fresh mercury drop from the HMDE had been exposed to a test solution for a given period of time, referred to in the following as the exposure time, t_{exp}, at a constant d.c. potential, E_i. All potentials were measured against a saturated calomel electrode (SCE). The d.c. voltage scan was started from E_i with the scan rates, v, of 98 mV s^{-1} for cyclic d.c. voltammetry and of 18 mV s^{-1} for a.c. voltammetry unless otherwise stated. Other details concerning the apparatus and methods of electrochemical measurements have been described elsewhere[1]

Results

Electrochemical measurements were performed at concentrations of FAD, C_{FAD}, lower than 3.6×10^{-6} mol dm^{-3}, at which the current due to the redox reaction of diffusing, unadsorbed FAD will be negligibly small compared with the current due to the surface redox reaction of FAD confined to the electrode surface by adsorption. The exposure time, t_{exp}, was varied from 0.5 to 5 min. In cyclic d.c. voltammetry FAD gave a pair of peak-shaped cathodic and anodic waves characteristic of the surface redox reaction at −0.40 V, which is attributable to the redox reaction of the isoalloxazine moiety.[1] The waves appeared in various shapes, depending on the exposure time and bulk concentration of FAD (Fig. 1), *i.e.*, on the surface concentration of FAD accumulated on the electrode surface during the exposure time. Figure 1 shows cyclic d.c. voltammograms of 2.7×10^{-6} mol dm^{-3} FAD, recorded after three different exposure times; the voltammograms A, B, and C were recorded at $t_{exp}=70$, 90, and 120 s, respec-

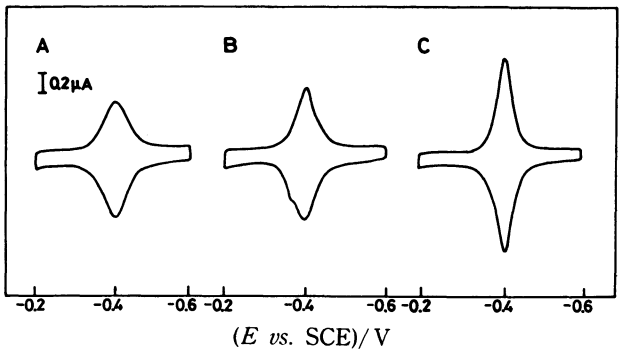

Fig. 1. Cyclic d.c. voltammograms of 2.7×10^{-6} mol dm^{-3} FAD recorded in a pH 6.9 phosphate buffer after three different t_{exp}'s at $E_i=-0.20$ V *vs.* SCE. t_{exp}: (A) 70 s, (B) 90 s, (C) 120 s.

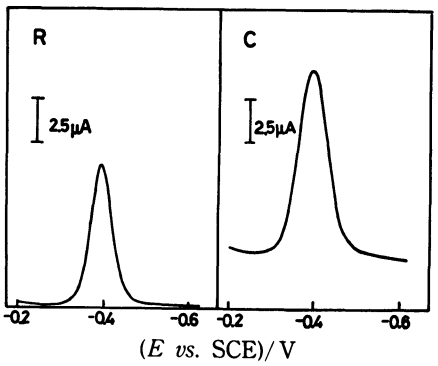

Fig. 2. A.c. voltammograms of 8.1×10^{-7} mol dm^{-3} FAD in a pH 6.9 phosphate buffer at 500 Hz. D.c. voltage scan was started from $E_i=-0.20$ V *vs.* SCE after $t_{exp}=$ 5 min. R Real component, C: imaginary component.

tively, at $E_i=-0.20$ V. In this study the surface concentrations of FAD, Γ, were estimated from the area under the cyclic d.c. wave (corrected for the base current) by assuming that the number of electron transferred for each molecule of FAD is equal to 2 and that $m_1/n_1=m_2/n_2=1$[5] or $m/n=1$.[6] When the surface concentration of FAD was lower than 5.0×10^{-11} mol cm^{-2}, the shapes of the cyclic d.c. waves were broadened and flattened as seen by voltammogram A in Fig. 1, of which Γ was estimated at 4.9×10^{-11} mol cm^{-2}. When Γ exceeded 5.0×10^{-11} mol cm^{-2} and approached 5.8×10^{-11} mol cm^{-2}, the waves became narrower and sharper (see voltammogram C in Fig. 1). In the intermediate surface concentrations of FAD, *i.e.*, 5.0×10^{-11} mol cm^{-2} $<\Gamma<5.8\times10^{-11}$ mol cm^{-2}, the wave shape was asymmetrical and deformed (see voltammogram B in Fig. 1) and changed sensitively with Γ. Quite interestingly the electrochemical behavior of the adsorbed FAD at $\Gamma<5.0\times10^{-11}$ mol cm^{-2} was different from that at $\Gamma>5.8\times10^{-11}$ mol cm^{-2}. In the following the surface concentration of FAD lower than 5.0×10^{-11} mol cm^{-2} will be referred to as the low surface concentration, whereas the surface concentration higher than 5.8×10^{-11} mol cm^{-2} will be referred to as the high surface concentration.

Cyclic d.c. and a.c. Voltammetric Behavior at the Low Surface Concentration. When $\Gamma<5.0\times10^{-11}$ mol cm^{-2}, *i.e.*, at the low surface concentration, the electrochemical behavior of FAD adsorbed on the HMDE was essentially the same[8] as that of FMN adsorbed on the HMDE.[1] In cyclic d.c. voltammetry, the peak heights of the cathodic and anodic waves, I_{pc} and I_{pa}, after correction for the base currents, were proportional to the potential scan rate, v, between 32 and 192 mV s^{-1}, and also to Γ at $\Gamma<5.0\times10^{-11}$ mol cm^{-2} (Fig. 3). The peak height ratio I_{pa}/I_{pc} was unity in the above-stated ranges of v and Γ when corrected for the difference between the amounts of the adsorbed FAD at the cathodic and anodic peak potentials due to the difference in t_{exp}. The peak potentials of the cathodic and anodic waves, E_{Pc}^{DC} and E_{Pa}^{DC}, coincided with each other and were independent of both v and Γ; $E_{Pc}^{DC}=E_{Pa}^{DC}=-0.40$ V. The half-peak widths of the cathodic and anodic waves, $\Delta E_{p/2.c}^{DC}$ and $\Delta E_{p/2.a}^{DC}$, were also independent within experimental errors of both v and Γ; $\Delta E_{p/2.c}^{DC}=\Delta E_{p/2.a}^{DC}=$ 70 ± 3 mV.

Figure 2 shows representative real and imaginary components of a.c. voltammograms of adsorbed FAD at $\Gamma<5.0\times10^{-11}$ mol cm^{-2}; the voltammograms were recorded after the electrode had been exposed to the electrolysis solution containing 8.1×10^{-7} mol dm^{-3} FAD for $t_{exp}=5$ min at $E_i=-0.20$ V, where Γ was estimated at 3.0×10^{-11} mol cm^{-2} from the cyclic d.c. wave measured under the same conditions. The peak potentials of the real and imaginary components, E_p^{real} and E_p^{imag}, were independent of the ac frequency in the range between 100 and 500 Hz, and also of Γ less than 5.0×10^{-11} mol cm^{-2}. They agreed with each other and with the peak potentials of the cyclic d.c. waves; $E_p^{real}=E_p^{imag}(=E_p^{AC})=-0.40$ V. The ratio of the peak height of the real component ($\delta_1 I_p^{real}$) to that of the imaginary component ($\delta_1 I_p^{imag}$), $(\delta_1 I_p^{real}/\delta_1 I_p^{imag})_{E=E_p^{AC}}$, was proportional to the a.c. frequency between 100 and 500 Hz.

Cyclic d.c. and a.c. Voltammetric Behavior at the High Surface Concentration. When Γ exceeded 5.8×10^{-11} mol cm^{-2}, *i.e.*, at the high surface concentration, the shape of the cyclic d.c. waves became narrower and sharper compared with those observed at the low surface concentration (see Fig. 1). Table 1 shows the scan rate dependence of the peak heights, peak potentials, and half-peak widths of the cyclic d.c. voltammograms. The voltammograms were recorded with various scan rates after the electrode had been exposed to 3.6×10^{-6} mol dm^{-3} FAD solution for $t_{exp}=2$ min at $E_i=-0.20$ V, when the surface concentration of FAD was estimated at 6.7×10^{-11} mol cm^{-2}. E_{Pc}^{DC} and E_{Pa}^{DC} agreed with each other and were independent of both v and Γ; $E_{Pc}^{DC}=E_{Pa}^{DC}(=E_P^{DC})=-0.40$ V. $\Delta E_{p/2.c}^{DC}$ and $\Delta E_{p/2.a}^{DC}$ were practically invariant with both v and Γ; $\Delta E_{p/2.c}^{DC}=\Delta E_{p/2.a}^{DC}=43\pm0.7$ mV. Both I_{pc} and I_{pa} were proportional to v (Table 1) and increased linearly with Γ at $\Gamma>5.8\times10^{-11}$ mol cm^{-2} as shown in Fig. 3. The peak height ratio I_{pa}/I_{pc} was unity independently of v and Γ.

The a.c. voltammetric behavior of adsorbed FAD at the high surface concentration was different from that at the low surface concentration described above. Figure 4 shows a.c. voltammograms of 3.6×10^{-6} mol dm^{-3} FAD at two a.c. frequencies, 100 and 500 Hz;

Table 1. Scan rate dependence of the peak current, peak potential and half-peak width of cyclic d.c. voltammograms of FAD adsorbed at the high surface concentration on mercury electrode at pH 6.9[a)]

Scan rate/mV s^{-1}	I_{pc}/μA	I_{pa}/μA	E_{Pc}^{DC}/V[b)]	E_{Pa}^{DC}/V[b)]	$\Delta E_{p/2,c}^{DC}$/mV	$\Delta E_{p/2,a}^{DC}$/mV
32	0.17	0.17	−0.40	−0.40	42	42
48	0.25	0.25	−0.40	−0.40	42	43
98	0.48	0.48	−0.40	−0.40	42	43
193	0.88	0.88	−0.40	−0.40	45	45

a) $C_{FAD}=3.6\times10^{-6}$ mol dm^{-3}, $t_{exp}=2$ min at $E_i=-0.20$ V *vs.* SCE. b) V *vs.* SCE.

Table 2. Peak potential and half-peakwidth of a.c. voltammograms of FAD adsorbed at the high surface concentration on mercury electrode at pH 6.9[a)]

Frequency/Hz	E_p^{real}/V[b)]		E_p^{imag}/V[b)]		$\Delta E_{p/2}^{real}$/mV		$\Delta E_{p/2}^{imag}$/mV	
	Obsd	Calcd[c)]	Obsd	Calcd[c)]	Obsd	Calcd[c)]	Obsd	Calcd[c)]
100	0.40_2	0.4019	0.39_8	0.3984	35	36.4	47	47.0
200	0.40_0	0.4003	0.39_2	0.3946	38	40.4	56	52.4
300	0.39_8	0.3987	0.38_8	0.3905	42	44.2	64	57.4
400	0.39_6	0.3973	0.38_5	0.3870	46	47.4	68	60.9
500	0.39_5	0.3963	0.38_3	0.3842	50	49.8	75	62.9

a) $C_{FAD}=3.6\times10^{-6}$ mol dm^{-3}, $t_{exp}=2$ min at $E_i=-0.20$ V *vs.* SCE($\Gamma=6.7\times10^{-11}$ mol cm^{-2}). b) V *vs.* SCE.
c) Calculated by using $E'_0=-0.400$ V *vs.* SCE, $k_{sap}=5.12\times10^2$ s^{-1}, $J=1.5$, $G=0.13$, and $\theta_t=0.957$.

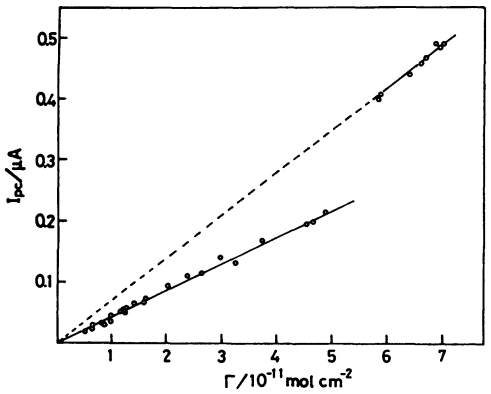

Fig. 3. Plot of I_{pc} against Γ at pH 6.9.

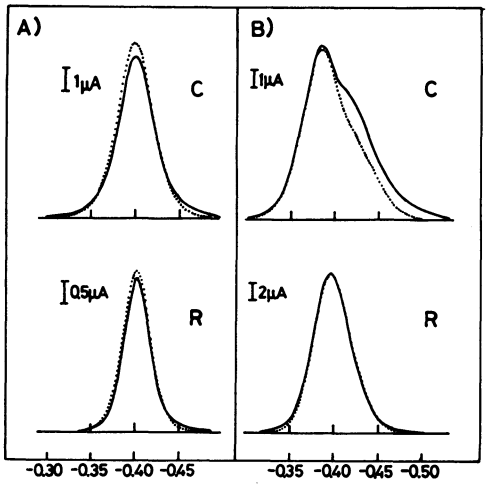

Fig. 4. A.c.voltammograms of 3.6×10^{-6} mol dm^{-3} FAD recorded after $t_{exp}=2$ min at $E_i=-0.20$ V *vs.* SCE at (A) 100 Hz and (B) 500 Hz. R: Real component, C: imaginary component. Dotted lines represent theoretical voltammograms calculated by Eqs. 5 and 6 using $E'_0=-0.400$ V *vs.* SCE, $k_{sap}=5.12\times10^2$ s^{-1}, $J=1.5$, $G=0.13$, $\theta_t=0.957$ and $\Gamma^{max}=7.0\times10^{-11}$ mol cm^{-2}.

the voltammograms were recorded after $t_{exp}=2$ min at $E_i=-0.20$ V, when Γ was estimated at 6.7×10^{-11} mol cm^{-2} from the corresponding cyclic d.c. wave. The peak potentials of the real and imaginary components shifted to a more positive potential with an increase in the a.c. frequency as shown in Table 2. In addition, the wave shapes, in particular, of the imaginary components changed from a nearly symmetrical to an asymmetrical one with a shoulder with increasing a.c. frequency. However, the current ratio of the real component to the imaginary one measured at $E=E_P^{DC}$, $(\delta_1 I_F^{real}/\delta_1 I_F^{imag})_{E=E_P^{DC}}$, was proportional to a.c. frequency as shown in Fig. 5.

Discussion

Adsorption of FAD on Mercury Electrode Surface. The cyclic d.c. voltammetric data given above indicate that both the oxidized and reduced forms of FAD are strongly adsorbed on the HMDE surface. Figure 6 shows the dependence of the cathodic peak height, I_{pc}, on t_{exp} at various concentrations of FAD. In this figure the points below the broken line correspond to the cyclic d.c. voltammograms at the low surface concentration, *i.e.*, at $\Gamma<5.0\times10^{-11}$ mol cm^{-2} (see Fig. 1A), whereas the points above the line correspond to the voltammograms at the high surface concentration, *i.e.*, at $\Gamma>5.8\times10^{-11}$ mol cm^{-2} (see Fig. 1C), and the points in parentheses correspond to the intermediate surface concentration between 5.0×10^{-11} and 5.8×10^{-11} mol cm^{-2}. At $C_{FAD}\leq1.08\times10^{-6}$ mol dm^{-3}, the peak height I_{pc} (and also I_{pa}) increased linearly with the

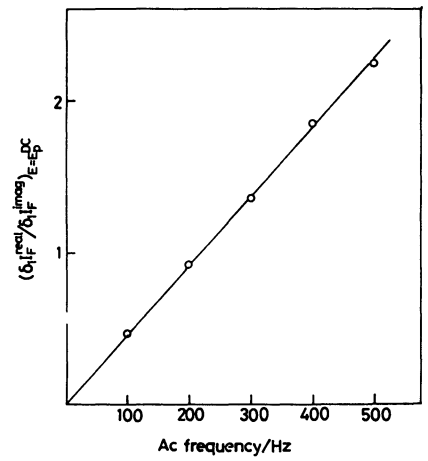

Fig. 5. Frequency dependence of the ac current ratio at $E=E_p^{dc}$, $(\delta_1 I_p^{real}/\delta_1 I_p^{imag})_{E=E_p^{dc}}$. A.c. voltammograms were recorded after the electrode had been exposed to 3.6×10^{-6} mol dm^{-3} FAD solution for $t_{exp}=2$ min at $E_i=-0.20$ V *vs.* SCE.

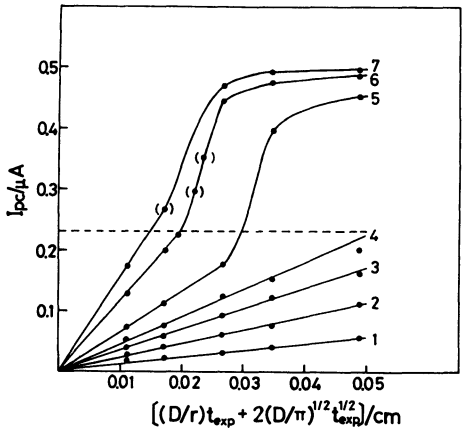

Fig. 6. Plot of I_{pc} against $[(D/r)t_{exp}+2(D/\pi)^{1/2}t_{exp}^{1/2}]$ at pH 6.9. Bulk concentrations of FAD in mol dm^{-3} are: (1) 2.7×10^{-7}; (2) 5.4×10^{-7}; (3) 8.1×10^{-7}; (4) 1.08×10^{-6}; (5) 1.62×10^{-6}; (6) 2.7×10^{-6}; (7) 3.6×10^{-6}.

$[(D/r)t_{exp}+2(D/\pi)^{1/2}t_{exp}^{1/2}]$ function, where D is the diffusion coefficient of FAD, which was estimated to be 2.4×10^{-6} cm^2 s^{-1} from the d.c. polarographic data, using the Ilkovič equation, and r is the radius of the HMDE, which was estimated to be 0.038 cm. In addition, the slopes of the linear plots were proportional to C_{FAD}. These results indicate the diffusion-controlled adsorption of FAD at the mercury electrode surface.[1,9] On the other hand, at $C_{FAD}\geq1.62\times10^{-6}$ mol dm^{-3}, as t_{exp} increased the wave shapes changed from a broad (see Fig. 1A) to a sharp one (see Fig. 1C) and the peak height I_{pc} increased and attained a maximum value, when Γ reached a maximum value, Γ^{max}. The Γ^{max} value was estimated to be 7.0×10^{-11} mol cm^{-2} from the cyclic d.c. voltammogram. If we assume that an FAD molecule is adsorbed on the electrode surface with its isoalloxazine ring plane parallel but its adenine ring plane vertical to the electrode surface, a CPK molecular model gives $\Gamma^{max}=7.5\times10^{-11}$ mol cm^{-2}. On the other hand, when both the ring planes are oriented parallel

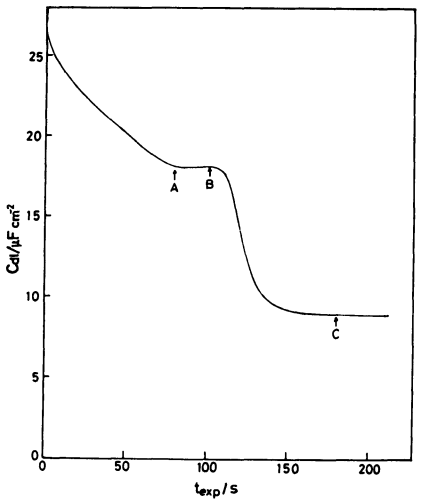

Fig. 7. t_{exp}-dependence of C_{dl} measured in 2.7×10^{-6} mol dm^{-3} FAD solution at -0.20 V *vs.* SCE at pH 6.9.

to the electrode surface, it gives $\Gamma^{max}=5.2\times10^{-11}$ mol cm^{-2}. These results suggest that at the low surface concentrations, *i.e.*, at $\Gamma<5.0\times10^{-11}$ mol cm^{-2} FAD molecule is adsorbed probably with both isoalloxazine and adenine ring planes oriented parallel to the electrode surface, and that, as the surface concentration of FAD exceeds 5.0×10^{-11} mol cm^{-2}, reorientation of the adsorbed FAD molecule occurs, resulting in an adsorbed FAD molecule probably with the isoalloxazine ring plane oriented parallel and the adenine ring plane oriented vertical to the electrode surface. This reorientation of the adsorbed FAD molecule should cause the observed transition in the voltammetric behavior of FAD at the HMDE.

The reorientation of the adsorbed FAD molecules was further indicated by the differential capacity measurement. Figure 7 shows the t_{exp}-dependence of the differential capacity, C_{dl}, at -0.20 V, where no faradaic current takes place, in 2.7×10^{-6} mol dm^{-3} FAD solution. Under these experimental conditions the surface concentrations of FAD at various t_{exp}'s were estimated from the corresponding cyclic d.c. voltammograms as: $\Gamma=5.0$, 5.8, and 6.9×10^{-11} mol cm^{-2} at $t_{exp}=$ 80, 100, and 180 s, respectively (marked by arrows A, B, and C, respectively, in Fig. 7). If the orientation mode of the adsorbed molecules remains unchanged in spite of an increase in Γ and if the relative decrease of the double layer capacitance is proportional to the surface concentration of the adsorbed molecules, then the double layer capacitance can be written as

$$C_{dl}=C_{dl}^{\circ}+(C_{dl}^{max}-C_{dl}^{\circ})(\Gamma/\Gamma^{max}), \quad (1)$$

where C_{dl}° and C_{dl}^{max} are the double layer capacitances in the absence of adsorbed FAD and at the maximum adsorption of FAD, respectively. That is, the double layer capacitance should decrease monotonically with the increase of Γ. Actually, for $t_{exp}<70$ s the decrease in the double layer capacitance, $\Delta C_{dl}=C_{dl}^{\circ}-C_{dl}$, was proportional to the $[(D/r)t_{exp}+2(D/\pi)^{1/2}t_{exp}^{1/2}]$ function as shown in Fig. 8, indicating the diffusion-controlled adsorption of FAD for $t_{exp}<70$ s. Substituting $\Gamma=[(D/r)t_{exp}+2(D/\pi)^{1/2}t_{exp}^{1/2}]C_{FAD}$ into Eq. 1, the slope of

the ΔC_{dl} *vs.* $[(D/r)t_{exp}+2(D/\pi)^{1/2}t_{exp}^{1/2}]$ plot can be given by $[(C_{dl}^{o}-C_{dl}^{max})\times C_{FAD}/\Gamma^{max}]$. If we assume that $C_{dl}^{max}=C_{dl}$ at $t_{exq}=80$ s and $\Gamma^{max}=5.0\times10^{-11}$ mol cm^{-2}, the slope can be calculated to be 4.6×10^{2} μF cm^{-3}, which agreed reasonablly well with the experimental value of 4.2×10^{2} μF cm^{-3} obtained from the plot in Fig. 8. These results show that the decrease of C_{dl} with t_{exp} at $t_{exp}<70$ s can be explained by the diffusion-controlled monolayer adsorption of FAD, approaching monotonically to the maximum adsorption near at $t_{exp}=80$ s or $\Gamma=5.0\times10^{-11}$ mol cm^{-2}, which is the maximum adsorption at the low surface concentration. At $t_{exp}>100$ s or $\Gamma>5.8\times10^{-11}$ mol cm^{-2}, C_{dl} decreased abruptly and approached a small value, approximately one half of the value at $\Gamma=5.0\times10^{-11}$ mol cm^{-2}, near at $t_{exp}=180$ s or $\Gamma=7.0\times10^{-11}$ mol cm^{-2}, which is the maximum adsorption at the high surface concentration. The decrease in the capacitance implies an increase in the effective thickness of the adsorbed FAD layer. This interpretation agrees with the above-stated reorientation mechanism of adsorbed FAD molecules when the surface concentration exceeds 5.8×10^{-11} mol cm^{-2}.

Surface Redox Reaction of FAD Adsorbed on the HMDE. A) Surface Redox Reaction at the Low Surface Concentration: As described above the cyclic d.c. and a.c. voltammetric behavior of the adsorbed FAD at the low surface concentration was essentially the same as that of the adsorbed FMN on the mercury electrode surface.[1] The behavior was explained also by the simplified equations[1,5] of the cyclic d.c. and a.c. voltammetry for a two-step surface redox reaction;

$$O_{ad} + e = S_{ad}$$
$$S_{ad} + e = R_{ad}. \quad (I)$$

The semiquinone formation constant, $K=[S_{ad}]^2/[O_{ad}][R_{ad}]$, was determined from the cyclic d.c. voltammograms as $K=1.5$ from $\Delta E_{p/2.c}^{DC}$ or $\Delta E_{p/2.a}^{DC}$ using Eq. 5 in Ref. 1 and $K=1.5$ from the slope of the I_{pc} *vs.* Γ plot (Fig. 3) using Eq. 6 in Ref. 1. The apparent (average) rate constants of the charge transfer, k_{sap}, were determined at several surface concentrations using Eq. 7 in Ref. 1. A linear dependence of ln k_{sap} on the surface coverage θ_t with a slope, a, of 1.0 was obtained, where $\theta_t\equiv\Gamma/\Gamma^{max}$ was estimated by taking $\Gamma^{max}=5.0\times10^{-11}$ mol cm^{-2}. The apparent rate constant at $\theta_t=0$, $k_{sap}(\theta_t\to0)$, was determined by the extrapolation of the ln k_{sap} *vs.* θ_t plot to $\theta_t=0$. Table 3 summarizes the values of the formal redox potential of the adsorbed redox couple O_{ad}/R_{ad}, E_o', as well as K, $k_{sap}(\theta_t\to0)$, Γ^{max}, and a. For reference the values of the electrochemical redox reaction parameters for the surface redox reactions of FMN[1] and riboflavin (RF)[8] at mercury electrode are also given in Table 3.

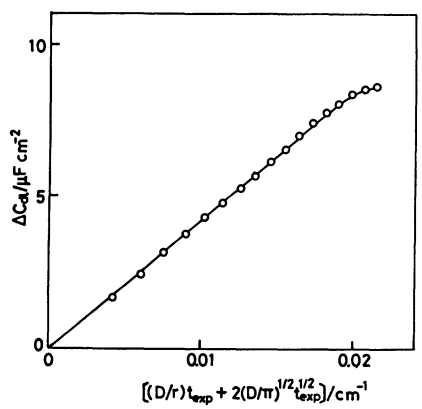

Fig. 8. Plot of ΔC_{dl} against $[(D/r)t_{exp}+2(D/\pi)^{1/2}t_{exp}^{1/2}]$ at pH 6.9. Data were taken from the results presented in Fig. 7.

Table 3. Electroche mical redox properties of flavins adsorbed on mercury electrode at pH 6.9

	RF[8]	FMN[1]	FAD[a]
$(E_o'$ *vs.*SCE)/V	−0.40	−0.41	−0.40
K	1.2	1.1	1.5
$k_{sap}(\theta_t\to0)/10^3$ s^{-1}	9.9	9.5	7.2
$\Gamma^{max}/10^{-11}$ mol cm^{-2}	8.9	8.0	5.0
a	2.0	1.3	1.0

a) Data obtained in this study at the low surface concentration (see text). Previous, less accurate data[8] on FAD were corrected as given here.

B) Surface Redox Reaction at the High Surface Concentration: As described above, at the high surface concentration, *i.e.*, 5.8×10^{-11} mol cm^{-2} $<\Gamma<7.0\times10^{-11}$ mol cm^{-2}, the half-peak widths of the cyclic d.c. waves were 43 mV, which suggest that the semiquinone formation constant K is very small. Therefore, the cyclic d.c. and a.c. voltammetric behavior of adsorbed FAD at the high surface concentration was interpreted in terms of a single-step two-electron surface redox reaction rather than a two-step one-electron surface redox reaction. According to the theory of cyclic d.c.[6,7] and a.c.[6] voltammetry for a single-step n-electron surface redox reaction,

$$O_{ad} + ne = R_{ad}, \quad (II)$$

in which the interactions between the adsorbed reactants are taken into account, the peak heights, I_{pc} and I_{pa}, the peak potentials, E_{Pc}^{DC} and E_{Pa}^{DC}, and the half-peak widths, $\Delta E_{p/2.c}^{DC}$ and $\Delta E_{p/2.a}^{DC}$, of the reversible cyclic d.c. voltammogram, and the real and imaginary components of the a.c. current, $\delta_1 I_F^{real}$ and $\delta_1 I_F^{imag}$, of d.c. reversible surface redox process can be written, for $\alpha=\beta=0.5$ and $n=m=2$ (see Ref. 6 for the details), as:

$$-I_{pc} = I_{pa} = (4F^2/RT)vA\Gamma_t(4-G\theta_t)^{-1} \quad (2)$$

$$E_{pc}^{DC} = E_{pa}^{DC} = E_o' = E_o + (RT/2F) \times[\ln(B_R/B_O) - (H\theta_t/2)] \quad (3)$$

$$\Delta E_{p/2.c}^{DC} = \Delta E_{p/2.a}^{DC} = (RT/F)|\ln(1+\gamma)/(1-\gamma) - (G\theta_t/2)| \quad (4)$$

$$\delta_1 I_F^{real} = 4(F^2/RT)\omega\Gamma_t A\delta_1 E \times \frac{\lambda\exp[-(G-J)\bar{f}\theta_t/2](1-\bar{f})^{3/2}\bar{f}^{3/2}}{\exp[-(G-J)\bar{f}\theta_t][1-G\theta_t(1-\bar{f})\bar{f}]^2+\lambda^2(1-\bar{f})\bar{f}} \quad (5)$$

$$\delta_1 I_F^{imag} = 4(F^2/RT)\omega\Gamma_t A\delta_1 E \times \frac{\exp[-(G-J)\bar{f}\theta_t][1-G\theta_t(1-\bar{f})\bar{f}]\bar{f}(1-\bar{f})}{\exp[-(G-J)\bar{f}\theta_t][1-G\theta_t(1-\bar{f})\bar{f}]^2+\lambda^2(1-\bar{f})\bar{f}}, \quad (6)$$

with

$$G = a_{OO} + a_{RR} - a_{OR} - a_{RO} \quad (7a)$$

$$H = a_{OO} - a_{RR} + a_{OR} - a_{RO} \quad (7b)$$

$$\gamma = [(4-G\theta_t)/(8-G\theta_t)]^{1/2} \quad (7c)$$

$$J = 2(a_{RR}-a_{RO}) \quad (7d)$$

$$\lambda = \omega/k_{sap} \quad (7e)$$

$$k_{sap} = k_s(B_O B_R)^{-1/2}\exp[-(a_{RR}+a_{OR})\theta_t/2], \quad (7f)$$

where B_i is the constant representing the adsorption energy of species i(i=O,R), a_{ij}(i,j=O,R) Frumkin's a-parameter of the interaction between the adsorbed species i and j, E'_o and E_o are the formal potentials of the adsorbed redox couple O_{ad}/R_{ad} and of the redox couple O/R in the bulk of solution, respectively, ω and $\delta_1 E$ are the angular frequency and amplitude of the applied a.c. voltage, respectively, $\bar{f}$ is the mean ("d.c.") ffraction of the surface coverage defined by $\bar{f}=\bar{\Gamma}_o/\Gamma_t(\Gamma_t=\bar{\Gamma}_o+\bar{\Gamma}_R)$, $\bar{\Gamma}_i$ being the mean ("d.c.") value of the surface concentration of species i, θ_t the total surface coverage defined by $\theta_t=\Gamma_t/\Gamma^{max}$, and A the surface area of the electrode. $\bar{f}$ is related to the d.c. potential, $E_{d.c.}$ by

$$E_{d.c.} = E'_o + (RT/2F)[\ln(\bar{f}/(1-\bar{f})) + (1-2\bar{f})G\theta_t/2]. \quad (8)$$

The interaction parameter G can be determined from the half-peak widths of the cyclic d.c. voltammograms (Eq. 4). Application of Eq. 4 to the experimental results gave the average value of G as 0.13 ± 0.02 in the range of Γ between 5.8×10^{-11} and 7.0×10^{-11} mol cm^{-2}, *i.e.*, $0.83\leq\theta_t\leq1.0$. This G value leads us to the normalized peak heights of the d.c. waves, $\Phi=-I_{pc}/4(F^2/RT)v\Gamma_t A = I_{pa}/4(F^2/RT)v\Gamma_t A$, of 0.257 at $\theta_t=0.83$ and of 0.258 at $\theta_t=1.0$, which means that the peak heights are practically proportional to Γ_t, *i.e.*,

$$-I_{pc} = I_{pa} \cong 0.257(4F^2/RT)v\Gamma_t A. \quad (2')$$

Thus the (theoretical) slope of the I_{pc} *vs.* Γ_t plot can be calculated using Eq. 2′ to be 7.1×10^3 A cm^2 mol^{-1}, which agreed well with the experimental value of 7.0×10^3 A cm^2 mol^{-1}. Equation 3 predicts a linear dependence of E_{Pc}^{Dc} or E_{Pa}^{Dc} on θ_t for $H\neq0$. However, since θ_t varied between 0.83 and 1.0, the dependence of E_{Pc}^{Dc} or E_{Pa}^{Dc} on θ_t would not be experimentally detectable when $|H|$ is not so large. For example, the difference in E_{Pc}^{Dc}'s between at $\theta_t=0.83$ and 1.0 is calculated to be 2.2 mV for $H=2$, which is well below the magnitude of experimental errors of the present determination. Thus we may conclude that the value of $|H|$ is not so large and should not exceed 2, which is a reasonable conclusion in view of Eq. 7.

Equations 5 and 6 predict that both the real and imaginary components are not symmetrical with respect to the E'_o-axis for $G\neq J$, that their peak potentials, E_p^{real} and E_p^{imag}, should shift positively for $G<J$ or negatively for $G>J$ with increasing a.c. frequency, and that the current ratio $(\delta_1 I_F^{real}/\delta_1 I_F^{imag})_{E_{d.c.}=E'_o}$ should be proportional to a.c. frequency:

$$(\delta_1 I_F^{real}/\delta_1 I_F^{imag})_{E_{d.c.}=E'_o} = \omega/2k_{sap}\exp[-(G-J)\theta_t/4](1-G\theta_t/4). \quad (9)$$

The linear dependence of current ratio on the a.c. frequency was experimentally found, as shown in Fig. 5. Table 2 gives the experimental and calculated values of E_p^{real}, E_p^{imag}, $\Delta E_{p/2}^{real}$, and $\Delta E_{p/2}^{imag}$ of the surface redox reaction of adsorbed FAD at the high surface concentration, where the calculated values were obtained using the following values of the parameters: $E'_o=-0.400$ V, $k_{sap}=5.12\times10^2$ s^{-1}, $J=1.5$ and $G=0.13$. The a.c. peak currents are plotted against the a.c. frequency in Fig. 9, in which the solid lines are drawn by Eqs. 5 and 6 using the same values of the parameters as above. In Fig. 4 the dotted curves represent the theoretical a.c. voltammograms calculated by using the same values of the parameters as above, which are compared with the experimental voltammograms shown as solid lines. The agreement between the theory and experimental results seems reasonably good, except for curves C in Fig. 4B, in which the experimental asymmetric wave form is reproduced only semi-quantitatively by the present theory. These results indicate that the essential features of the cyclic d.c. and a.c. voltammetric behavior of adsorbed FAD at the high surface concentration can be reproduced by the theory of a single-step surface redox reaction in which the interaction between the adsorbed molecules are taken into account. It is interesting that the orientation mode of the adsorbed FAD molecules has a significant influence on the electrochemical properties of the surface redox reaction of FAD, such as the semiquinone formation constant and the charge transfer rate constant.

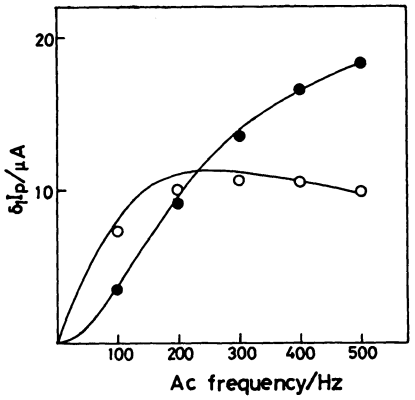

Fig. 9. Dependence of the a.c. peak heights of 3.6×10^{-6} mol dm^{-3} FAD on a.c. frequency at pH 6.9. A.c. voltammograms were recorded after $t_{exp}=2$ min at $E_i=-0.20$ V *vs.* SCE. ●: Real component, ○: imaginary component. Solid lines represent theoretical curves calculated by Eqs. 5 and 6 using the same values of the parameters as used in Fig. 4.

References

1) T. Kakutani, K. Kano, S. Ando, and M. Senda, *Bull. Chem. Soc. Jpn.*, **54**, 884 (1981).
2) L. Gorton and G. Johansson, *J. Electroanal. Chem. Interfacial Electrochem.*, **113**, 151 (1980).
3) H. Huck, *Ber. Bunsenges. Phys. Chem.*, **85**, 221 (1981).
4) H. Huck, *Z. Phys. Chem. NF*, **120**, 39 (1980).
5) T. Kakutani and M. Senda, *Bull. Chem. Soc. Jpn.*, **53**, 1942 (1980).
6) T. Kakutani and M. Senda, *Bull. Chem. Soc. Jpn.*, **52**. 3236 (1979).

7) E. Laviron, *J. Electroanal. Chem. Interfacial Electrochem.*, **52**, 395 (1974).
8) T. Kakutani, I. Katasho, S. Ando, and M. Senda, Paper presented at the annual meeting on polarography and electroanalytical chemistry, Oct. 17—18th, 1981; abstract, *Rev. Polarogr. (Kyoto)* **27**, 92 (1981).
9) J. Koryta, *Collect. Czech. Chem. Commun.*, **18**, 206 (1935).